Journal of Plant Biology, October 2006, 49(5) : 376-383

Changes in the Plastid Ultrastructure during *Sedum rotundifolium* Leaf Development

In Sun Kim*
Biology Department, College of Natural Sciences, Keimyung University, Daegu 704-701, Korea

The ultrastructure of plastids was investigated in succulent leaves of *Sedum rotundifolium* to examine their changes during development. Leaves were categorized as etiolated, immature, young, and mature, based on their developmental stage and size. Of particular interest were the features of the tubular inclusion bodies (TIBs) and starch grains. These, along with vacuole size, showed remarkable changes over time. Etioplasts of unexposed leaves had prolamellar bodies, abundant starch grains, large TIB, few plastoglobuli, and thylakoid systems. Membranes of the thylakoids were still continuous with those of the prolamellar body. The plastids were often influenced by the presence and profile of inclusion bodies and starch grains throughout the early stages. Morphology was highly variable in the etioplasts but consistently hemispherical or ovoid in mature chloroplasts. TIB was most abundant in the etiolated leaves, but disappeared completely with development. Starch grains also became significantly reduced in size. Both young and mature mesophyll cells exhibited a normal chloroplast ultrastructure and huge central vacuoles, with an extremely thin peripheral cytoplasm. Grana were extensive and comprised a large portion of the chloroplasts. Traces of peripheral reticulum were also discovered in the chloroplasts of expanded leaves. The implications of these ultrastructural changes in the tubular inclusions and starch grains are discussed with relevance to Crassulacean acid metabolism (CAM).

Keywords: CAM, mesophyll, plastid ultrastructure, *Sedum rotundifolium*, tubular inclusion bodies

Crassulacean acid metabolism (CAM), a water-conserving photosynthetic pathway, is a mode of plant adaptation to water-stressed habitats. Its distinctive features include the nocturnal fixation of CO_2 via phosphoenol pyruvate carboxylase (PEPcase), the accumulation of organic acids in the vacuole, and subsequent diurnal deacidification of CO_2 via ribulose-1,5-biphosphate carboxylase/oxygenase (Rubisco) during photosynthesis. In CAM plants, those two enzymes, PEPcase and Rubisco, are present in all chloroplast-containing chlorenchyma cells where such a night-and-day photosynthetic pattern occurs. Thus, the regulation of enzyme activity is temporal rather than spatial, with PEPcase being active in the dark and Rubisco only in the light (Leegood, 1999). Further, the expression of its many components is very sensitive to biological and environmental factors (Winter and Smith, 1996a; Leegood et al., 1997; McDonald, 2003). Generally, CAM plants have mesophyll that is not differentiated into palisade and spongy parenchyma layers. These traits are important under water-limiting conditions (Kluge and Ting, 1978).

Distinctive anatomical characteristics associated with CAM plants are succulence at the cellular level, which is manifested by large, thin-walled cells with huge vacuoles for the storage of organic acids in the leaves and stems. Tissue succulence is defined by a low ratio of surface area to volume and a high capacity for water storage, resulting in high tissue water potentials even under stressed conditions (Bowyer and Leegood, 1997). Only those succulents with large water storage vacuoles that are accompanied by chloroplasts in the same cells are considered CAM plants (Kluge and Ting, 1978). In typical succulents or CAM plants, the chlorenchyma occurs directly beneath the epidermis (Gibson, 1982), showing very thin primary walls, conspicuous intercellular spaces, and numerous chloroplasts located peripherally to a large central vacuole. CAM requires this close proximity between the large vacuole and the chloroplasts to accommodate the diurnal fluxes in organic acids between these two intracellular structures (Kluge and Ting, 1978). The vacuole typically occupies over 90% of the chlorenchyma cell volume in CAM plants. A greater capacity for CAM with increasing leaf age has been suggested as a predictable feature in most leaf succulents (Osmond, 1978; Ting and Rayder, 1982; Winter and Smith, 1996a).

The genus *Sedum* in the Crassulaceae contains succulent species adapted to dry environments. Species in this genus primarily exhibit the CAM mode (Kluge and Ting, 1978; Griffiths, 1988; Smith and Winter, 1996). Such plants are usually well adapted to survival under drought. Although they generally live in habitats where they must withstand diurnal and seasonal periods of alternating wet and very dry conditions (Gibson, 1982; Smirnoff, 1996), not all CAM species are found in arid environments; in fact, many, such as the *Sedum rotundifolium* examined in this study, occur in the xeric microenvironments of mesic regions (Guralnick et al., 1986; Smirnoff, 1996). *S. rotundifolium*, which shows daily acid fluctuations (data not shown), grows on rocky surfaces or in very thin soil in the mesic environment of Mt. Juwang, Korea.

The anatomical structure of CAM plants is generally defined by its simplicity, but ultrastructural studies of their chloroplasts have revealed various types of inclusion bod-

*Corresponding author; fax +82-53-580-5305
e-mail botany@kmu.ac.kr

Abbreviations: c, chloroplast; cw, cell wall; g, grana; is, intercellular space; p, plasmodesmata; pl, prolamellar body; s, starch grain; tib, tubular inclusion body; v, vacuole; Figure 1-6, 10-17, transmission electron micrographs; Figure 7-9, high voltage transmission electron micrographs.

ies, such as tubules or tubule-like structures in the stroma (Kim, 1997). Tubules have been observed in the chloroplasts of several CAM plants (Salema and Brandao, 1978; Santos and Salema, 1981, 1983; Kim, 1997), whereas others contain tubular inclusion bodies (TIB) in their chloroplasts, especially when they are young (Thompson et al., 1977; Kim, 1997). *Sedum* species also possess such inclusions in their chloroplasts (Brandao and Salema, 1974; Santos and Salema, 1983; Kim, 1997). However, little research has been conducted on the ultrastructural changes in plastids during leaf development in these CAM plants, particularly with respect to the presence and properties of TIB. Furthermore, no detailed studies on the developmental changes to the plastid ultrastructure in *Sedum* species have yet been reported. Hence, the objective of this investigation was to expand our knowledge of this species by examining the plastids at four different leaf stages in Korean endemic *S. rotundifolium*.

MATERIALS AND METHODS

Plants of mature *S. rotundifolium* D. Lee (1996) were collected in September and October of 2003 and 2004 from Mt. Juwang (ca. 720.6 m), Gyeongsangbuk-do, Korea. Leaves from 5 to 10 plants were removed at each node, proceeding downward on the stem. The following leaf stages were sampled for electron microscopy: 1) unexposed, small leaves just developed from the leaf primordia, pale yellow and ca. 1 mm long; 2) 5- to 7-mm-long immature, pale-green leaves near the shoot apex; 3) 15- to 20-mm-long young, green leaves; and 4) 40- to 45-mm-long mature, healthy leaves. For light and transmission electron microscopy (TEM), the sampled tissues (unexposed through fully expanded leaves) were processed immediately, as follows: ca. 1- to 2-mm pieces were dissected and fixed in 3% glutaraldehyde for 3 h at room temperature, followed by post-fixation in 2% osmium tetroxide for 2 to 4 h at 4°C. The fixatives were buffered with and the fixed tissues were washed three times each in 0.1 M potassium phosphate at pH 7.2 (Kim and Fisher, 1990; Kim, 1997). All tissues were then dehydrated through an acetone series and embedded in Spurr resin. Afterward, 60- to 90-nm ultrathin sections were prepared with a Reichert (Germany) 7000 ultramicrotome, using a diamond knife. These sections were placed on meshed copper grids coated with 0.35% chloroform-diethanol formvar solution, then stained with 2% uranyl acetate (UA) and 1% lead citrate for 30 to 45 min each. Finally, the grids were examined with an Hitachi (Japan) H-7000 TEM, operated at 60 to 100 kV. For the high voltage electron microscopy (HVEM), tissues were fixed in glutaraldehyde and osmium tetroxide, as described above. After osmication and rinsing in buffer, the specimens were soaked in aqueous 1% UA in a mealate buffer for 2 h at 4°C. They were then dehydrated in an acetone series, infiltrated overnight in a resin mixture, and embedded in Spurr resin. 0.2- to 1.0-µm-thick sections were mounted on formvar-coated copper slot grids and stained with 5% UA in 70% methanol for 1.5 h at 60°C, then in lead citrate for 30 min at 25°C. Finally, the grids were carbon-coated to enhance stability during examination using a Hitachi H 1250-M HVEM, operated at 1000 kV. For the optical diffraction analysis, the sections were tilted in the electron microscope and electron micrographs were recorded on Kodak (USA) EM plates, first at a magnification of 65,000. The analysis was then performed on an optical bench built in the facility at Keimyung University. The diffraction patterns were obtained using screened electron micrographs of the recorded crystalline inclusion bodies as diffraction subjects in a modified Lipson (USA) optical diffractometer.

RESULTS

Light Microscopy

The mesophyll in mature *S. rotundifolium* leaves was continuous from the abaxial to the adaxial epidermis, and did not differentiate into palisade and spongy parenchyma. It comprised thin-walled parenchyma cells that were largely isodiametric. No bundle sheath was formed around the vascular tissue, nor was any sclerenchyma detected. The mesophyll cells did not present any unusual or distinctive features at the light-microscopic level, except in their intercellular spaces. In the mesophyll tissue only, differences were noted between immature and mature leaves, with the former exhibiting a low volume of air space, while, in the latter, the relative leaf volume occupied by air space was significantly higher. Increases in vacuole size, and in the amount and size of inclusion bodies and starch grains in the mesophyll plastids, differed remarkably throughout leaf development. The most interesting feature was the occurrence of plastid TIB in the earlier stages. Ultrastructural changes in these plastids during growth are characterized below.

Electron Microscopy

Mesophyll cells in the unexposed and smallest leaves developed etioplasts similar to those found in plants grown in the absence of light. These etioplasts were scattered throughout dense cytoplasm where various cellular organelles were dispersed along small vacuoles (Fig. 1). Mitochondria were numerous and closely associated with the etioplasts. Microbodies were also common in the cytoplasm (Fig. 2). Plasmodesmata were numerous in the walls of neighboring cells during the early stages (Fig. 3). The etioplasts contained prolamellar bodies, abundant starch grains, prominent TIB, few plastoglobuli, and a thylakoid system (Fig. 4). The prolamellar body, a semi-crystalline lattice of a membranous system, often constituted a small portion of the etiolated plastids. Membranes of the thylakoid system were still continuous with those of the prolamellar body. Arrays of TIB frequently occupied a large volume (up to 40 or 50%) of the plastids, at times nearly extending throughout the stroma (Fig. 4). In some cases, the TIB appeared to be attached to the inner etioplast envelope on one side and to the thylakoids on the other (Fig. 5), even though they were separated from the structures. However, no spatial relationship was detected between the TIB and prolamellar body. The TIB appeared as paracrystalline aggregates in transverse sections (Fig. 6, 7), while both paracrystalline and paralleled

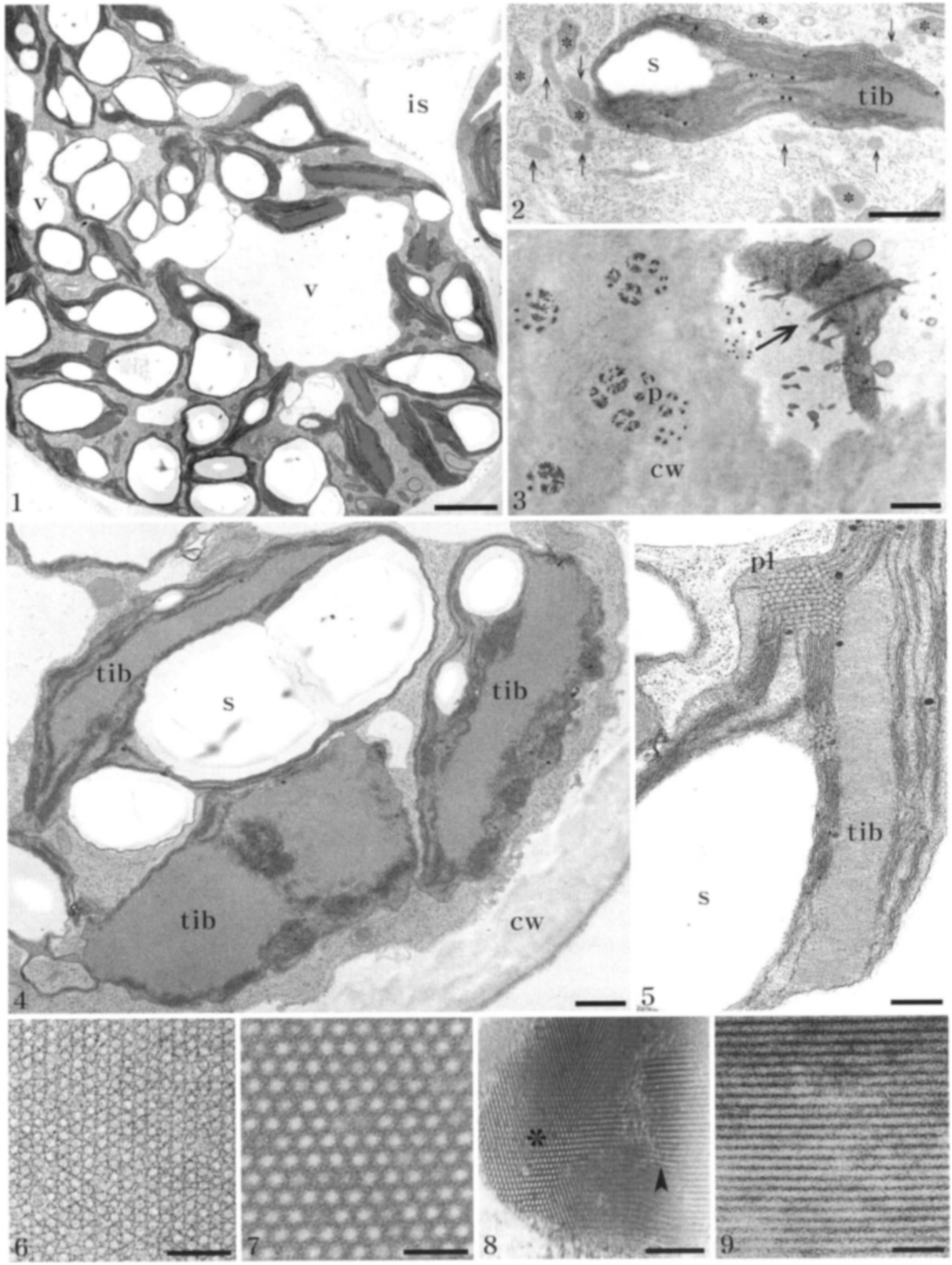

Figure 1-9. 1, Immature mesophyll cell from etiolated leaf, exhibiting dense cytoplasm, vacuoles of various sizes, and small intercellular spaces. Bar = 5 μm; 2, Etioplast closely associated with mitochondria (asterisks) and microbodies (arrows). Bar = 1 μm; 3, Oblique section through cell wall showing clusters of plasmodesmata where intercellular transport may occur (arrow). Bar =1 μm; 4, Prominent TIB and starch grains occupying large portion of plastid. Bar = 1 μm; 5, TIB neighboring a prolamellar body on one side and inner plastid membrane on the other, in parallel fashion. Bar = 0.5 μm; 6, Transverse section of TIB exhibiting paracrystalline arrangement. Bar = 100 nm; 7, Transverse section (0.25-μm-thick) of TIB demonstrating paracrystalline arrangement. HVEM. Bar = 50 nm; 8, Portion of TIB showing paracrystalline (asterisk) and paralleled elements (arrowhead) within single aggregate. HVEM. Bar = 1.5 μm; 9, Longitudinal section of TIB clearly demonstrating paralleled tubular elements. HVEM. Bar = 100 nm.

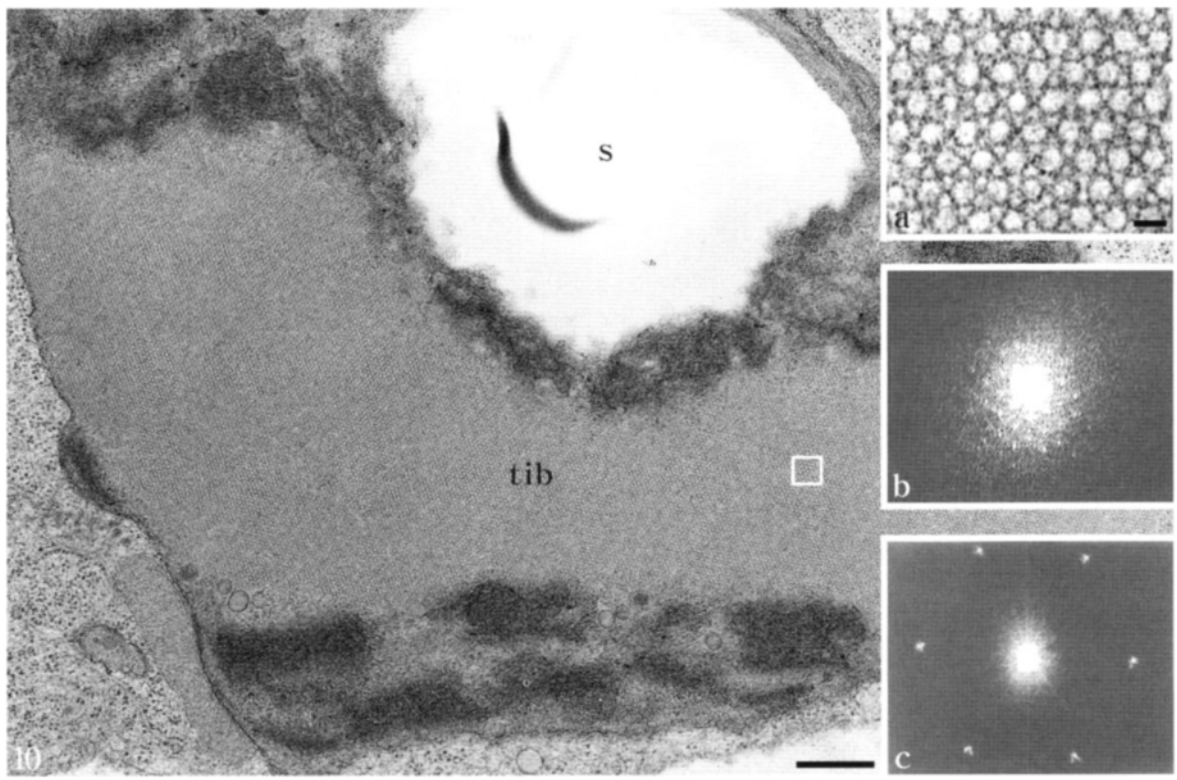

Figure 10. Transverse section of plastid showing paracrystalline TIB in etiolated leaf. Bar = 0.5 μm. Inset a, close-up of boxed area showing central hexagons with six equilateral triangles. Bar = 20 nm. Inset b, c, optical diffraction pattern from electron micrograph of paracrystalline structure in Figure 10.

tubular arrangements were seen within a single aggregate when examined by HVEM (Fig. 8). The patterns of elements exhibiting both paralleled and paracrystalline arrangements within one TIB were of particular interest. In a longitudinal section, paralleled elements were well-demonstrated (Fig. 9), sometimes several microns long. The hexagonal arrangement of those elements was obvious in the transverse sections of thin- and thick-sectioned specimens. In the paracrystalline TIB (Fig. 10), the plane approximately at a right angle to the structure's long axis consisted of a network of tubular elements, each of which was made up of a central hexagon with an observed face-to-face distance of 18 to 20 nm. A starlike pattern of hexagons formed where each face was subtended by six equilateral triangles (Fig. 10a). Optical diffraction analysis of these paracrystalline TIB (Fig. 10b, c) showed a strong hexagonal pattern. The number of thylakoids and grana increased with the subsequent disappearance of the prolamellar body as the plastids developed.

In the mesophyll cells of immature leaves, a large central vacuole had already formed in some cells (Fig. 11), while others were still undergoing gradual vacuolization through the fusion of several smaller vacuoles (Fig. 12). Mitochondria and microbodies were relatively common in the cytoplasm of cells with plasmodesmata. Other prominent structures that distinguished the plastids included the TIB and starch grains, as was seen in the etiolated leaves. The shapes of the plastids were often influenced by the presence and profile of the TIB and starch grains within (Fig. 11). Some TIBs nearly extended the entire length, while being partially enclosed by thylakoids (Fig. 12). A relatively large volume of plastids, usually <20% based on the serial sections, was still occupied by the TIB at this stage (Fig. 13). The TIB also demonstrated either paracrystalline (Fig. 14) or paralleled plate-like structures (Fig. 15), depending on the sectioning angle. Mesophyll cells at this stage had already taken on the succulent feature.

As their development progressed, cells of the young and mature leaves experienced a dramatic increase in size, with very few organelles visible in any one section. The cells had large central vacuoles with very thin cytoplasm. Over 95% of the cell volume was occupied by the vacuole in their mesophyll. A transformation from the highly variable structure in the etioplast stage to the consistently hemispherical or ovoid mature chloroplasts occurred as the leaves expanded (Fig. 16, 17), and mesophyll chloroplasts at these stages exhibited a normal ultrastructural organization. Grana were extensive, comprising a large portion of the chloroplast volume. Starch grains were much smaller as the chloroplasts matured; this was particularly evident in older leaves, where tiny grains were seen in many of the chloroplasts (Fig. 17). Endoplasmic reticulum and ribosomes were the most common elements within the extremely thin cytoplasm of the mesophyll cells. Distribution of the plasmodesmata was scarce between adjacent cells, and no TIB were seen in their chloroplasts. In general, those chloroplasts observed beyond the younger stages exhibited well-developed grana, plastoglobuli, and occasional traces of peripheral reticulum. The incidence of that peripheral reticulum in the chloroplasts of younger leaves was less frequent than in those of

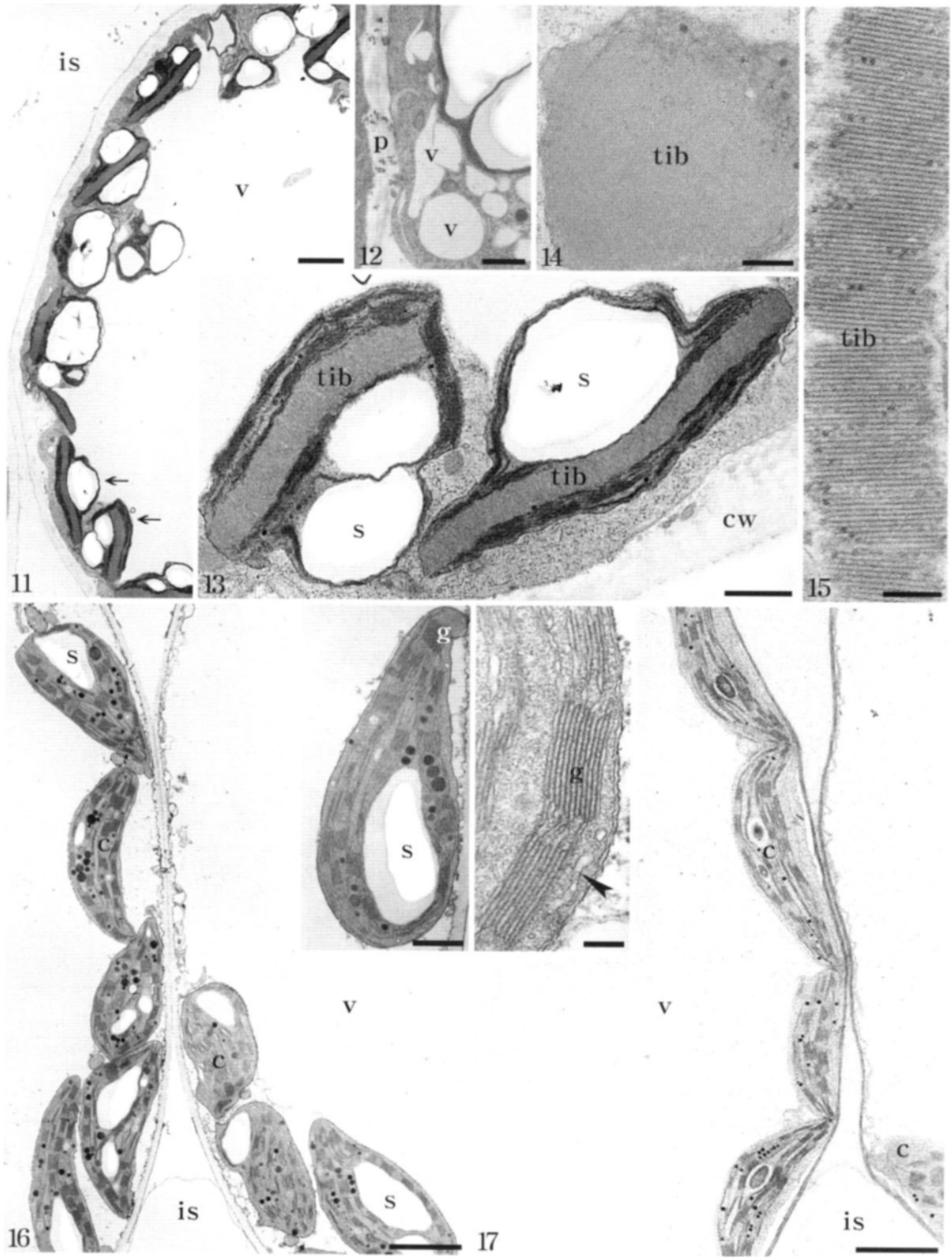

Figure 11-17. 11, Developing mesophyll cell from immature leaf with large central vacuole and thin peripheral cytoplasm. Arrowed plastids are detailed in Figure 13. Bar = 3.0 μm; 12, Progression of gradual vacuolization by fusion of various-sized vacuoles in immature leaf. Note the plasmodesmata in cell wall. Bar = 1 μm; 13, High magnification of plastids (arrows) from Figure 11. Plastids are irregular in shape due to TIB and starch grains. Bar = 1.0 μm; 14, Transversely sectioned plastid showing paracrystalline TIB. Bar = 0.3 μm; 15, Part of longitudinally sectioned plastid showing paralleled plate-like TIB. Bar = 0.5 μm; 16, Numerous chloroplasts in mesophyll cells of young leaf, located peripherally to huge central vacuole. Reduced starch grains are apparent. Bar = 3.0 μm. Inset, mature chloroplast with grana, plastoglobuli, and starch grain. Bar = 1.0 μm; 17, Mesophyll cells of mature leaf showing peripherally arranged chloroplasts with grana and reduced starch grains. Bar = 3.0 μm. Inset, traces of peripheral reticulum (arrowhead) and well-developed grana within stroma. Bar = 0.1 μm.

fully expanded, matured leaves. Phytoferritin, which has been reported in some succulent species, was not detected in *S. rotundifolium* chloroplasts.

DISCUSSION

An ultrastructural investigation was performed on four different developmental stages of succulent leaves in *S. rotundifolium*, with an emphasis on features of TIB in the plastids. The mesophyll in mature leaves consisted of isodiametric, water-storing cells, each containing a large central vacuole bounded by a thin, peripheral layer of cytoplasm. The presence of numerous chloroplasts in these mesophyll cells is characteristic of CAM plants. In typical CAM succulents, chlorenchyma occurs directly beneath the epidermis, and cells usually have a very thin primary wall and conspicuous intercellular spaces. They also contain numerous enlarged chloroplasts located peripherally to a large central vacuole. CAM requires such close proximity of a large vacuole to chloroplasts in order to accommodate the diurnal fluxes of organic acids between them (Kluge and Ting, 1978). The cytoplasmic area occupied by the vacuoles increased as the leaves developed. Once a vacuole is formed, it presumably grows during cell differentiation. Here, an increase in vacuole area along a row of cells suggested that relative growth of the vacuole exceeded that of the cells during differentiation. This could have been a result of either the continuous formation of new vacuoles or an increase in the size of established vacuoles. Such an enlargement was especially evident during differentiation in this species (Fig. 11). The vacuoles, closely located to numerous chloroplasts in both young and mature leaves of *S. rotundifolium*, occupied about 90 to 95% of the chlorenchyma cell volume, as has also been reported with other CAM plants (Winter and Smith, 1996a).

Mesophyll cells of the etiolated leaves manifested the features of etioplasts seen in plants grown in darkness. The etioplasts, which represent a blocked stage along the path to chloroplast development (Waters and Pyke, 2005), clearly showed prolamellar bodies, starch grains, TIB, small plastoglobuli, and the thylakoid system (Fig. 5). However, the prolamellar body often constituted only a small portion of the etiolated plastids in *S. rotundifolium*. The morphological transition from etioplast to chloroplast involves the growth of plastids and progression of the prolamellar body into a thylakoid membrane system (Fosket, 1994; Newcomb, 1997; McDonald, 2003). Plastids undergo limited development in etiolated leaves (Gunning and Steer, 1996), and the proteins involved in chloroplast development are generally absent or are present only in very low amounts. Under darkness, the prolamellar body apparently forms as a result of the continued synthesis of thylakoid lipids, without a parallel synthesis of thylakoid proteins (Gunning and Steer, 1996). Here, most of the plastids in the etiolated and immature leaves were amorphous in their appearance due to the presence and shape of the TIB and starch grains. This suggests that they underwent extensive changes in their shape in succeeding stages.

A considerable reduction in the size of starch grains was observed during *S. rotundifolium* leaf development. However, although starch in the chloroplasts of CAM plants was previously identified as the likely carbon source for the synthesis of organic acids, other researchers have since determined that only small amounts of the carbon are actually derived from starch (cf., Black et al., 1996). For CAM to function, nocturnal acid accumulation must be balanced by a substantial carbohydrate supply. Because a major portion of the stored carbohydrate accumulates as soluble sugars rather than insoluble starches, as in many CAM species (Winter and Smith, 1996a), the abundant, large starch grains found here in the early stages probably played a larger role in plastid development rather than in the functioning of CAM. However, it is also highly possible that the early stages may have undergone photosynthetic pathways other than CAM. A gradual shift from C_3 to CAM occurs during leaf development, and maximal CAM activity is expressed only in mature leaves in some constitutive CAM plants (Winter and Smith, 1996b). Another feature noted during this current study was the proximity of thylakoids to any available starch grains. Thylakoids usually appeared closely appressed to the grains, especially in the early stages. However, it is yet to be answered whether this reflects that starch grains develop near one another or merely as an incidental juxtaposition. Furthermore, researchers must still investigate any possible correlation between the two during plastid differentiation.

Another distinct feature here was the disappearance of TIB in chloroplasts at later stages. Huge aggregates of tubules in hexagonal arrays were found in the stroma of the etioplasts. Non-membrane bounded tubular arrays, unrestricted to the plastid periphery, were present in large portions of these plastids. These inclusions, which were often very large, reaching several microns in length, have previously been recorded in *Sedum* species (Kim, 1997), and have been described in the plastids of several CAM plants (Thomson and de Journett, 1970; Lee and Thompson, 1973; Thomson and Platt, 1973; Brandao and Salema, 1974; Thompson et al., 1977; Salema and Brandao, 1978; Santos and Salema, 1981, 1983; Vaughn and Wilson, 1981; Rivera and Arnott, 1982; Kim, 1997). The dynamic and structural roles of the TIB and a possible relationship between them and CAM activity have been investigated in various studies (Brandao and Salema, 1974; Salema and Brandao, 1978; Santos and Salema, 1981, 1983). A possible link between the TIB and the onset of CAM has been strongly speculated because the TIB disappear with the initiation of CAM activity under certain experimental conditions (Thompson et al., 1977; Salema and Brandao, 1978; Santos and Salema, 1981).

The photosynthetic organs of most CAM plants have a succulent morphology, with high water-storing capacities that aid their survival in dry environments with an insufficient water supply. Strong and positive correlations between leaf succulence and the occurrence and magnitude of CAM have been reported in the Crassulaceae (Gibson, 1982; Winter and Smith, 1996a). Many CAM plants engage in a certain amount of daytime CO_2 uptake directly via C_3 photosynthesis (Osmond et al., 1996). The developmental state and prevailing environmental conditions affecting this pho-

tosynthetic functioning vary substantially by CAM species (Winter and Smith, 1996a). The phenomenon of succulent plants shifting from C_3 photosynthesis to CAM when stressed is now well-documented (Winter and Smith, 1996b). Furthermore, studies have revealed that this environmentally induced change from C_3 to CAM is accompanied by a very large increase in the activity of PEPcase and other enzymes (Guralnick and Ting, 1988; Winter and Smith, 1996b). Some members of the Crassulaceae show a shift in their response to drought, resulting in the switchover from C_3 to a more CAM-like metabolism (Ting and Rayder, 1982). A well-known example is *Kalanchöe innata*, where young leaves fix CO_2 by the C_3 photosynthetic pattern while older leaves fix CO_2 via CAM (Thompson et al., 1977). There, the changeover from C_3 to CAM activity in young *Kalanchöe* leaves coincides with the disappearance of the TIB, a phenomenon also noticed in this study. Thus, it may be possible to link the presence of TIB in *S. rotundifolium* to photosynthetic functioning. Currently, the most attractive hypothesis that accounts for the occurrence of plastid inclusion bodies in *S. rotundifolium* is that TIB in the etiolated and the immature leaves are involved in the storage of enzymes necessary for the operation of CAM in mature leaves.

Whether these inclusions are required at certain stages of cell development or whether they appear in response to specific environmental conditions awaits further elucidation. Moreover, studies of ultrastructural differentiation within additional CAM-performing *Sedum* species and their C_3 relatives are needed to better establish whether the structural attributes discussed here do indeed relate to certain photosynthetic pathways.

ACKNOWLEDGEMENTS

This work was supported by a Korea Research Foundation Grant (KRF-2003-070-C00037). The author thanks Dr. Tatsuo Arii of NIPS at Okazaki National Institutes of Natural Sciences, Japan, for providing the facilities, including the H 1250-M HVEM, and for technical assistance during this study.

Received May 22, 2006; accepted September 11, 2006.

LITERATURE CITED

Black CC, Chen JQ, Doong RL, Angelov MN, Sung SJS (1996) Alternative carbohydrate reserves used on the daily cycle of Crassulacean acid metabolism, *In* K Winter, JAC Smith, eds, Crassulacean Acid Metabolism. Springer, Berlin, pp 31-45

Bowyer JR, Leegood RC (1997) Photosynthesis, *In* PM Dey, JB Harborne, eds, Plant Biochemistry. Academic Press, New York, pp 49-110

Brandao I, Salema R (1974) Microtubules in chloroplasts of a higher plant (*Sedum* species). J Submicr Cytol 6: 381-390

Fosket DE (1994) Plant Growth and Development. Academic Press, New York, pp 274-279

Gibson AC (1982) The anatomy of succulence, *In* IP Ting, M Gibbs, eds, Crassulacean Acid Metabolism. Proceedings of the Fifth Annual Symposium in Botany, American Society of Plant Physiologists, Rockville, pp 1-17

Griffiths H (1988) Crassulacean acid metabolism: A re-appraisal of physiological plasticity in form and function, *In* JA Callow, ed, Advances in Botanical Research. Vol 15, Academic Press, London, pp 43-92

Gunning BES, Steer MW (1996) Plant Cell Biology: Structure and Function. Jones and Bartlett, Boston, pp 1-60

Guralnick LJ, Ting IP (1988) Seasonal patterns of water relations and enzyme activity of the facultative CAM plant *Portulacaria afra* (L.) Jacq. Plant Cell Environ 11: 811-818

Guralnick LJ, Ting IP, Lord EM (1986) Crassulacean acid metabolism in the Gesneriaceae. Amer J Bot 73: 336-345

Kim IS (1997) Chloroplast microtubules in young leaves of *Sedum rotundifolium*. J Plant Biol 40: 115-119

Kim IS, Fisher DG (1990) Structural aspects of the leaves of seven species of *Portulaca* growing in Hawaii. Can J Bot 68: 1803-1811

Kluge M, Ting OP (1978) Crassulacean Acid Metabolism. Springer-Verlag, Berlin, pp 10-107

Lee RE, Thompson A (1973) The stromacentre of plastids of *Kalanchöe pinnata* Persoon. J Ultrastruct Res 42: 451-456

Lee YN (1996) Flora of Korea. Kyo-Hak, Seoul, pp 271

Leegood RC (1999) Carbon dioxide concentrating mechanisms: C_4 photosynthesis and Crassulacean acid metabolism, *In* PJ Lea, RC Leegood, eds, Plant Biochemistry and Molecular Biology. John Wiley and Sons, New York, pp 51-79

Leegood RC, von Caemmerer S, Osmond CB (1997) Metabolite transport and photosynthetic regulation in C_4 and CAM plants, *In* DT Dennis, DH Turpin, DD Lefebvre, DB Layzell, eds, Plant Metabolism. Addison Wesley Longman, Harlow, pp 341-369

McDonald MS (2003) Photobiology of Higher Plants. John Wiley and Sons, Chichester, pp 100-147

Newcomb W (1997) Plastid structure and development, *In* DT Dennis, DH Turpin, DD Lefebvre, DB Layzell, eds, Plant Metabolism. Addison Wesley Longman, Harlow, pp 255-259

Osmond CB (1978) Crassulacean acid metabolism: A curiosity in context. Annu Rev Plant Physiol 29: 379-414

Osmond CB, Popp M, Robinson SA (1996) Stoichiometric nightmares: Studies of photosynthetic O_2 and CO_2 exchanges in CAM plants, *In* K Winter, JAC Smith, eds, Crassulacean Acid Metabolism. Springer, Berlin, pp 15-30

Rivera ER, Arnott HJ (1982) Tubular structures in the plastids of *Echinomastus intertextus* Brit. & Rose (Cactaceae). New Phytol 90: 551-561

Salema R, Brandao I (1978) Development of microtubules in chloroplasts of two halophytes forced to follow Crassulacean acid metabolism. J Ultrastruct Res 62: 132-136

Santos I, Salema R (1981) Chloroplast microtubules in some CAM plants. Bol Soc Brot 53: 1115-1122

Santos I, Salema R (1983) Stereological study of the variation of chloroplast tubules and volume in the CAM plant *Sedum telephium*. Z Pflanzenphysiol 113: 29-37

Smirnoff N (1996) Regulation of Crassulacean acid metabolism by water status in the C_3/CAM intermediate *Sedum telephium*, *In* K Winter, JAC Smith, eds, Crassulacean Acid Metabolism. Springer, Berlin, pp 176-191

Smith JAC, Winter K (1996) Taxonomic distribution of Crassulacean acid metabolism, *In* K Winter, JAC Smith, eds, Crassulacean Acid Metabolism. Springer, Berlin, pp 427-436

Thompson A, Vogel J, Lee RE (1977) Carbon dioxide uptake in relation to a plastid inclusion body in the succulent *Kalanchöe pinnata* Persoon. J Exp Bot 28: 1037-1041

Thomson WW, de Journett R (1970) Observations on inclusion bodies in subsidiary cells of *Opuntia* species. J Ultrastruct Res 31: 439-443

Thomson WW, Platt K (1973) Plastid ultrastructure in the barrel

cactus, *Echinocactus acanthodes*. New Phytol 72: 791-797
Ting IP, Rayder L (1982) Regulation of C_3 to CAM shift, *In* IP Ting, M Gibbs, eds, Crassulacean Acid Metabolism. Proceedings of the Fifth Annual Symposium in Botany, American Society of Plant Physiologists, Rockville, pp 193-207
Vaughn KC, Wilson KG (1981) Improved visualization of plastid fine structure: Plastid microtubules. Protoplasma 108: 21-27
Waters M, Pyke K (2005) Plastid development and differentiation, *In* SG Möller, ed, Plastids. Blackwell, Oxford, pp 30-59
Winter K, Smith JAC (1996a) An introduction to Crassulacean acid metabolism: Biochemical principles and ecological diversity, *In* K Winter, JAC Smith, eds, Crassulacean Acid Metabolism. Springer, Berlin, pp 1-13
Winter K, Smith JAC (1996b) Crassulacean acid metabolism: Current status and perspectives, *In* K Winter, JAC Smith, eds, Crassulacean Acid Metabolism. Springer, Berlin, pp 389-426